Carpathian Journal of Earth and Environmental Sciences, February 2021, Vol. 16, No. 1, p. 67 – 75; Doi:10.26471/cjees/2021/016/156

MICROPOROSITY CHANGES WITH ACIDIZING EFFECT IN SANDSTONES (KIZILDERE FORMATION-HATAY/S-TURKEY)

Melda AVCU[1] & Meryem YEŞİLOT KAPLAN[2]

[1]*İskenderun Technical University, Institute of Engineering and Sciences, TR-31200 İskenderun, Hatay*
[2]*İskenderun Technical University, Department of Oil and Natural Gas Engineering, TR-31200 İskenderun, Hatay*
meryem.yesilotkaplan@iste.edu.tr

Abstract: This study aims to determine the field and petrographic properties of sandstones observed in Arsuz-İskenderun (Hatay) region and micro-size porosity changes in acidizing stages. The fine-grained sandstones of the Aktepe formation have more quartz grains than the other components and the binding material is matrix. Rock fragments that consist of fossil shells, limestone and igneous fragments are observed relatively to quartz and feldspar grains in the Kızıldere formation sandstones. The first step of reservoir rock acidizing is HCl acidizing and the process is experimentally provided by capillarity experiment. HCl with dilution rates of 7.5% - 15% - 30% was absorbed into the samples at room temperature and after 100 minutes, effective distances were observed as 0.6-0.8-1.1 cm and dissolved rock amounts as 32.82-34.02-35.54 g, respectively. In acidizing process, the average porosity analysed with Micro-CT is 39.6% of acidified samples with 15% diluted acid and non-acidified samples, equivalent results were obtained with porosity values measured by well logs. There is an increase in the porosity of about 16% with acidizing. Pores were bonded together by acidizing and pore size increase about 20%. The change in the pore throat by acidizing is 105%. Calculation of porosity of rocks by Micro-CT and image processing methods can be performed faster compared to the other methods.

Keywords: Porosity, Micro-CT, Acidizing Effect, Kızıldere formation, Aktepe formation, Image processing.

1. INTRODUCTION

Reservoir characterization is a technique involving quantitative distribution of reservoir properties, such as porosity, permeability, and fluids saturations. The most important factors affecting the reservoir quality are microscopic pore structures (pore size and shape, pore size distribution, pore connection) that can be characterized by various methods.

Porosity is the most important petrophysical property of a reservoir rock. Pore abundance (storage capacity) and connectivity (permeability) are routinely used to characterize reservoirs in terms of their economical value, and as a means of assessing diagenetic alteration (Moore & Wade, 2013). Porosity and permeability variations for each diagenetic facies should be determined from routine core analyses to prepare a key for reservoir quality prediction. Whereas conventional porosity models focus on the macroscopic pores in sandstones (Archie, 1950; Wyllie & Rose, 1950), new researches show that most sandstones host vastly more complicated pore systems, particularly at the micrometer scale (Dong & Blunt 2009; Liu et al., 2017; Chen et al., 2020). Porosity and microporosity is an important research topic for several economic reasons. Micropores can host significant volumes of oil and gas, particularly when the hydrocarbon column is thick enough to overcome the entry pressure of the small pore throats.

Nowadays, significant research studies have been directed on pore-scale morphologies and sizes in sandstone reservoirs (Shabaninejad et al., 2018; Yang et al., 2019). The application of various techniques including X-ray computer tomography (XCT; Larmagnat et al., 2019; Feng et al., 2004; Peng et al., 2012), X-ray diffraction (XRD) analysis, thin sections, scanning electron microscopy (SEM; Hillier, 1994; Desbois et al., 2011), nuclear magnetic

resonance (NMR; Lai et al., 2016), high-pressure mercury injection (HPMI; Liu et al., 2018; Gao et al., 2019), and porosity and permeability measurements have provided important insights about the microscopic pore throat structure of sandstones (Xi et al., 2016; Wang et al., 2017; Cai et al., 2020).

Acidizing, one of the oldest well-stimulation techniques, is generally initiated when near wellbore formation damage causes a reduction in the productivity of an oil or gas reservoir. It is a relatively simple stimulation technique that has become one of the most cost-effective method to improve the well productivity and hence the hydrocarbons recovery significantly. During matrix acidizing, the acids dissolve the sediments and mud solids within the pores that are inhibiting the permeability of the rock and this process enlarges the natural pores of the reservoir which stimulates the flow of hydrocarbons. Experimental investigation of acidification of porosity changes is usually carried out with hydrochloric/hydrofluoric acid, but different acid types are also used.

Acidizing process consists of preflush, main acidizing, postflush and final flush. As pad-acid during sandstone acidizing, HCl is mainly used to remove carbonate and other mineral components in sandstone to expand pore throat. HCl pre-flushing of the formation, varying between 7.5% to 15%, dissolves carbonates and pushes the formation brines containing K, Na, Ca ions away from the wellbore.
Both medical and micro CT-scanning (Micro-CT) has been commonly used for decades for core analyses in order to analyse porosity, fractures, or assess fluid flow in porous rocks. Computed tomography (CT-Scanning) has been regularly applied to core analyses in wells, however there is still a need for improved porosity and porosity distribution in the entire pore scale spectrum, from the tens of nanometer to the meter-scale. Medical and Micro CT-scanning techniques, non-destructive methods, offer the possibility to quantify internal structures based on the measurement of X-Rays attenuation coefficients, which depend on the chemical composition and physical density of the materials analysed (Cnudde & Boone, 2013).

One of the Micro-CT usage types is to create and interpret the pore map by determining the three-dimensional pore structure, pore properties and pore areas. The pore network is determined from the pore map and the fluidity and transport processes are evaluated. The pore network system is effective in solving flow deformation problems in the size of microns (Yuan et al., 2015).

The operation method of the Micro-CT device is to convert the image from the scanner to three-dimensional data from two-dimensional images. The basis of digital image processing is based on computer algorithms. Analysis programs such as ImageJ, MATLAB, ICY, Avizo, Image Pro, ImageJ which convert images obtained by Micro-CT method into digital data are widely used (Grove & Jerram, 2011; Yang et al., 2014).

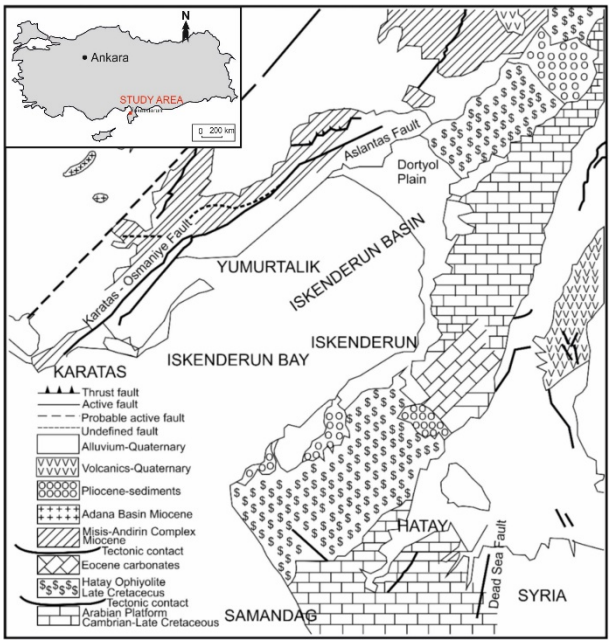

Figure 1. Location and geological map (Yalcin et al, 2019).

The major goals of this paper are to observe the effects of acidizing process, which is widely used in the oil and gas industry, on the effective porosity in a micro dimension and to determine the effect time of acids at different concentrations in sandstones. For this purpose, acid treatment changes in different concentrations were observed on the sandstones whose petrographic properties were determined and the acid effect and porosity were examined by comparing the acidified sample with the acidified sample in micro size. Porosity values obtained in Micro-CT and image processing programs are compared for accuracy and consistency. Microporosity changes of different concentrations of HCl acid have not been studied in literature yet. This paper examining porosity changes through capilarity will be useful and innovative both in field acidizing processes and in the literature. The study area is located in Arsuz and İskenderun districts (Fig. 1). In the study, the sandstones considered as a reservoir rock were used in Kızıldere Formation in Arsuz (Hatay) region.

2. GEOLOGICAL SETTING

The study area is located in Arsuz-İskenderun (Hatay) region and all stratigraphic units observed in

this region are of Miocene-Quaternary age. Iskenderun Bay, located in a graben, has large geological time periods of units (Cambrian-Recent) in Iskenderun and its surroundings. The Amanos Mountains are located between the Anatolian Plate and the Arabian Plate and north of the African Plate in terms of plate tectonics. These lithological units are overlain by Mesozoic limestones and ophiolitic rocks. These units are overlained by Paleocene-Eocene limestones and Middle Miocene shales and limestones. The autochthonous units forming the Amanos Mountains in the İskenderun basin are Paleozoic aged sandstones and green schists. Middle Miocene shales were deposited on Pre-Miocene basement rocks and ophiolitic rocks. The Kalecik formation, which is formed by the coarse clastics (Miocene), unconformably overlies the units.

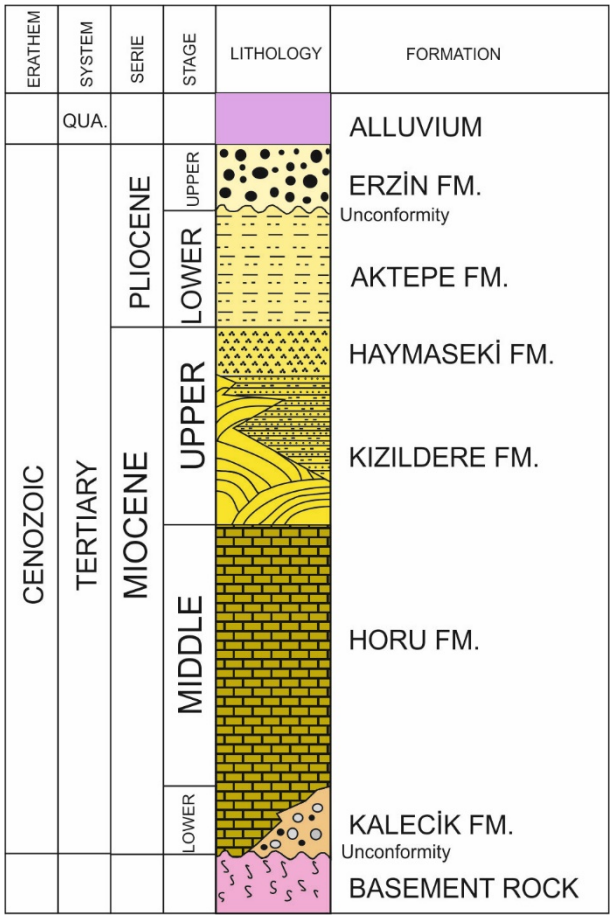

Figure 2. Generalized stratigraphic column section of Iskenderun Bay and surroundings (Tekin et al., 2006)

The Kalecik formation is conformably overlain by the Horu formation, while the Horu formation is overlain by sandstone-shale sequence in conformity with Kızıldere formation. On top of the Kızıldere formation, there is the Haymanseki formation, which is composed of evaporites. Aktepe formation conformably overlies on the Haymanseki formation while Erzin formation unconformably overlies Aktepe formation. The alluvials at the top are placed inconformity on all the units (Tendam, 1951; Schmidt, 1961; Kozlu, 1987). Lithostratigraphic units within the study area in İskenderun are Kızıldağ ophiolite, Kalecik formation Horu formation, Kızıldere formation, Haymaseki formation, Aktepe formation, Erzin formation and alluvium (Fig.2, Tekin et al., 2010).

Kızıldere Formation*:* Kızıldere formation, named first by Schmidt (1961), consists of sandstone claystone and lenticular reef limestones. It is unconformably overlain by the Aktepe formation, which is in conformity with the Menzelet formation under the Kızıldere formation. The age of the Kızıldere Formation is determined by Kozlu (1997) as Middle-Late Miocene and the thickness of formation is in the range of 800-2500 meters. Kızıldere Formation consists of a gray sequence, medium to thick bedded sandstone and gray, thin-bedded shales. Kozlu (1997) found the presence of carbonized plants in the formation and İztan & Harput (1988) reported formations containing organic matters. As a result of the trace element and TOC (Total Organic Carbon) experiments in their studies, Kılınç & Yeşilot Kaplan (2018) indicated that the Kızıldere formation can be deposited under anoxic environmental conditions and produces hydrocarbons.

Aktepe Formation: The unit formed during the Messinian time period and the transgression after the sea regression (Tekin et al., 2010). The Aktepe formation (Lower Pliocene) was determined by Kozlu (1997) as a sequence of light gray claystone, sandstone, siltstone with an average thickness of 200 meters.

3. MATERIALS AND METHODS

Sandstone and claystone samples were taken for analysis from the Aktepe and Kızıldere sandstone-claystone sequences and stratigraphic sections were measured in the field. Lithological and tectonic features of the region were studied.

The sandstone samples, taken from the sequence of sandsone-claystone in order to determine the petrographical properties of sandstones, were prepared in thin section laboratory of Istanbul Technical University. The thin sections were studied by polarized light microscopy and images were recorded to determine the grain size, grain shape, cement and intergranular properties of sandstones. As a result of the petrographic studies, it was decided to investigate the porosity changes on the samples with calcite cement.

Acidizing and capillarity tests were performed to determine the porosity changes with micron-size acid effects. Capillary test and then acidizing test were performed on the sandstone samples. Sample acidizing was first carried out at room temperature with 7.5-15-30 wt.% HCl on sandstones and the absorbed acid quantity was determined through the difference between the initial weight and the weights measured periodically. Water was then poured on the lower surface of the samples to observe the movements of the liquid in the sample from bottom to top by capillarity, their masses were measured at specified time and graphs of comparison of obtained values were plotted. Samples were weighed at 1, 4, 9, 16, 25, 36, 49, 64, 81, 100 minutes according to the capillarity test standarts.

The Micro-CT analysis was performed in at METU Biomaterials and Tissue Engineering Research Laboratory in order to observe porosity and internal structure changes after acidizing, acidified and non-acidified samples and to obtain 2D and 3D images. The variation of X-ray reflections was observed throughout the samples. The pore-size distributions and pore-throat analysis evaluated in this study are constructed with Micro-Computed Tomography (Micro-CT) imaging. Resolution for scanned samples is 13 μm/voxel and sample sizes are approximately 1 cm^3 in this study.

All processing of Micro-CT images was performed with ImageJ software and an open-source software. FIJI contains all the features of standard ImageJ software, but is modified with many plugins to make it more useful for analysis of 3D image stacks, such as those output from Micro-CT. ImageJ and FIJI are widely considered as the best free software for image analysis, mostly due to availability of a wide variety of plugins.

4. RESULTS AND DISCUSSION

4.1 Field Observations

The samples were taken from the formations that consist of claystone and sandstone sequence in the field. The sandstone-claystone sequence thickness is approximately 165 cm and generally medium bedded sandstones are observed (Aktepe formation) in the region. The thickness of claystones varies between 20 cm and 33 cm, while the thickness of sandstones is between 25 cm and 40 cm (Fig. 3A). The gray claystone – sandstone sequences is inclined to the south and have conchodial fracture surfaces. The claystones -dark gray on the outside, light gray on the inside surfaces- have a lot of cracks. Sandstone samples are reddish gray and medium bedded and alteration surfaces are observed. Abrasion surfaces observed in abundant cracked sandstones are relatively dark red and the abundant cracked and dark gray claystones are sequenced with sandstones. The outer surface of the dark gray sandstone has traces of oxidation and weathering marks are common in abundant cracked sandstone with medium layers (Fig. 3B).

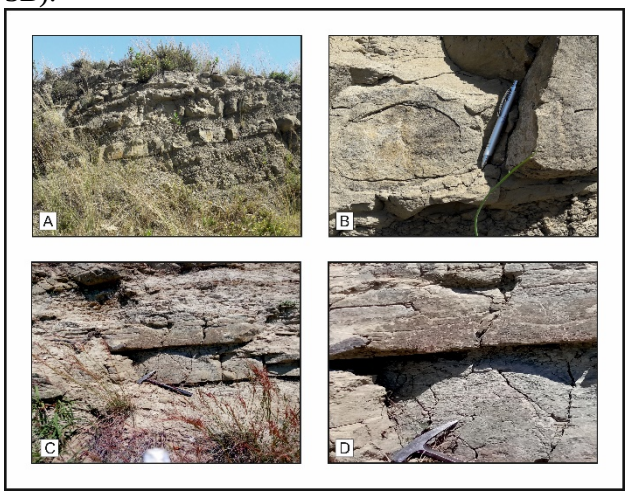

Figure 3. A) Sandstone-claystone sequence, B) Cracks and decomposition observed in sandstones of the Aktepe formation sandstones; C) sequence of thin-bedded claystones and medium-bedded sandstones; D) tectonic cracks frequently observed in sandstones of Kızıldere formation sandstones.

The lithological unit which indicates reservoir rock characteristics in Arsuz and İskenderun regions is the Kızıldere formation (Middle-Late Miocene). The Kızıldere formation that may be reservoir rock, contains sandstone and claystones sequences, and these claystones are known to be hydrocarbon source rocks. In the upper part of the formation, there are caprock consisting of evaporites and tectonic cracks which are common in all units in the region (Fig. 3.C-D). Sandstone and claystone sequences in the formation are common, the thickness of gray-yellow sandstones is between 10-50 cm and medium-thick bedded, gray colored claystones are between 2-30 cm and thin-medium bedded (Kılınç & Yeşilot Kaplan, 2019). Evaporitic units are sequenced with marls, and it is possible to find traces of organic matter in sandstones, claystones and marls.

4.2. Petrography

The quartz grains contain predominantly in fine-grained sandstones of Aktepe formation, other components such as feldspar and rock fragments are rarely observed (Fig. 4.A-B). Feldspar grains are equal in size with quartz grains (15-30 μm) and the feldspar grains with medium to good roundness are

generally plagioclase grains.

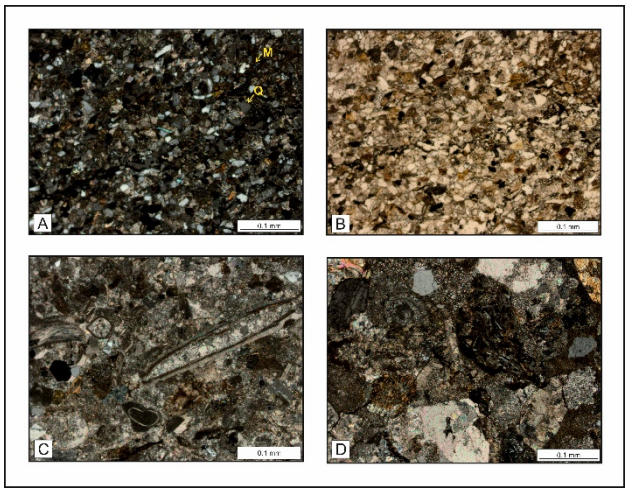

Figure 4. Microscopic view of sandstone in Aktepe and Kızıldere formation sample; A) polarized light appearance of Aktepe formations (Q = Quartz; M = Matrix), B) normal light appearance of Aktede formations, C) the rock fragments observed in sandstones of Kızıldere Formation (polarized light) Figure D) bioclasts in sandstones of Kızıldere formation (polarized light).

Rock fragments are usually mica grains and opaque minerals. Although calcite cement is observed between some grains, the binder material is usually matrix and it is present in approximately 20% and is named as sandstone “quartz vake”. Rock fragments such as fossil shells, limestone grains and igneous rock fragments are observed relatively more compared to quartz and feldspar grains. The sorting of grains is poor and all grains are angular (Fig. 4.C). The cement is calcite and named as “litharenite”. Claystones with sequentially observed sandstones are derived from basic-ultrabasic rocks in the Kızıldere formation (Fig. 4.D). The grain size is variable (20 µm to200 µm); however, the common grain size is between 120-200µm.

4.3. Capillarity and Acidizing Tests

It is possible to start a well into hydrocarbon production or to increase the amount of hydrocarbon during production by matrix acidizing. Acidizing process takes place by pumping, but the acid entering the well penetrates into the formation depending on the capillarity of the formation. Two experiments were designed to determine the amount of acid effect; capillarity and acidizing experiments. Capillarity experiment was performed with pure water in order to calculate the loss of substance during acidizing. In order to determine the effect of water and diluted HCl acid at certain time intervals, measurements were performed on the precision scales and these changes are given in Table 1.

The most commonly used acid dilution rates in the field acidizing processes are 7.5 %, 15% and 30% hydrochloric acid. In Table 2, the volumes, surface areas and the minimum and maximum effect amounts of diluted acid are listed for the samples used in the three types of acidification in the experiment. The dissolved rock particles, together with the consumed acid, move away from the sample by the effect of gravity. The amount of mass measured at specified times cannot be used to determine the amount of dilute acid due to the dissolved rock particles, so the capillarity test was also performed. Graphs of the mass changes in the sample and time during acidizing and capillarity experiments are given in Figure 5. Hydrochloric acid was consumed after the start of the experiment (7.5% HCl for 25 min.; 15% HCl for 36 min. and 30% HCl for 25 min., respectively).

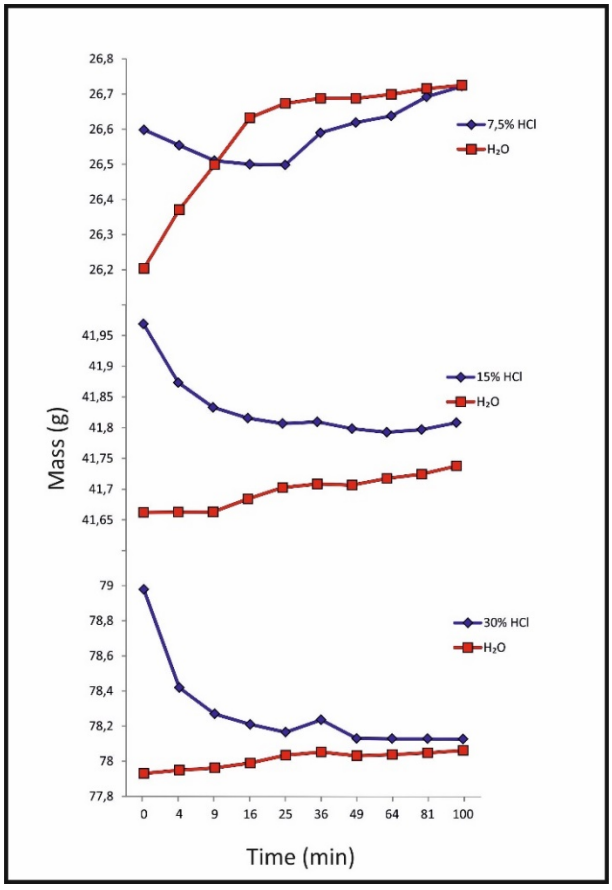

Figure 5. Time-dependent mass change graphs of acidizing and capilarity experiments

4.4. Micro-CT Images

Samples were prepared for the Micro-CT assay with and without acidizing and capillarity tests. Firstly, the sandstone sample was dissolved with 15% diluted hydrochloric acid and then the 1.5 cm surface area containing the acidified and non-acidified zones

Table 1. Time/mass relationship of samples in capillarity and acidizing experiments

ACIDIZING EXPERIMENT				CAPILLARITY EXPERIMENT		
Time (min)	KD-12- A7.5	KD-12- A15	KD-12- A30	KD-12 A7.5	KD-12- A15	KD-12- A30
0	26.5982	41.9689	78.9777	26.2032	41.6620	77.9306
4	26.5540	41.8733	78.4182	26.3705	41.6626	77.9488
9	26.5102	41.8330	78.2686	26.4988	41.6629	77.9621
16	26.5001	41.8155	78.2090	26.6324	41.6840	77.9897
25	26.4983	41.8067	78.1649	26.6733	41.7025	78.0345
36	26.5898	41.8094	78.2354	26.6879	41.7083	78.0517
49	26.6190	41.7982	78.1290	26.6877	41.7066	78.0311
64	26.6376	41.7925	78.1274	26.6990	41.7173	78.0377
81	26.6921	41.7968	78.1276	26.7157	41.7244	78.0474
100	26.7218	41.8080	78.1250	26.7251	41.7376	78.0609

Table 2. Sizes of samples used in experiments and acid effect volumes

Dilution Rate	Sample sizes-width/length/height (cm)	Sample Volume (cm^3)	Average Acid Effect Distance (cm)	The Amount of Solute (g)	The Influence of Acid Volume (cm^3)
7.5%	4.6/2.9/2.9	38.686	0.6	32.8180	21.34
15%	4.5/2.5/2.6	29.25	0.8	34.0243	22.50
30%	4.6/4.5/4.5	93.15	1.1	35.5433	51.75

A

was analyzed by using Micro-CT scanner. The change of the acid effect in the acidified sample depending on the capillarity directions is shown in Figure 6. The other sample (K-12) is not acidified and its surface size is 1.5 cm.

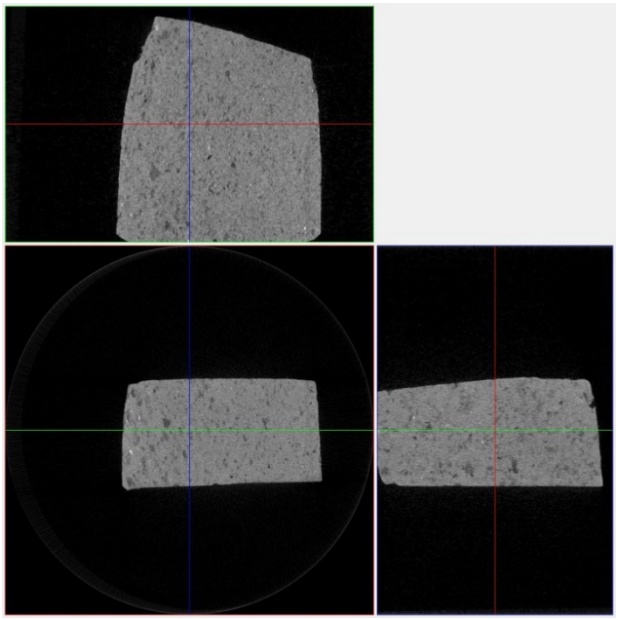

Figure 6. Three-axis cross-section of acidified sandstone sample with Micro-CT scanning.

It is possible to analyze the open, closed and total porosity volumes of the samples by Micro-CT method. difference in porosity was observed between the acidified sample (K-12) and the non-acidified sample (K-12-A-15) in this method. Accordingly, while the percentage of open porosity was 35.461% in the non-acidified sample, it increased to 39.539% in the other sample with the effect of acidizing, an increase of 11% was calculated. The percentage of closed porosity was 4.223% in the non-acided sample and was measured as 2.418% in the acided sample after the opening of the pores with acidizing. The total porosity values were 38.187% in the non-acided sample and 41.001% in the acided sample porosity value in the acidized sample shows that acidizing causes an increase of about 2.8% in porosity values.

The regions, where the grains other than porosity are scanned, are calculated as "percentage object volume" in Micro-CT analysis. The object volume percentage was measured as 58.99% in acided sample while this ratio was 61.81% in the non-acided sample. The object volume percentage decreased by 2.8% with the effect of HCl acid diluted 15%.

4.5. Calculation of Porosity with Image Processing

The porosity properties of the images taken from a distance of micron size are determined in FIJI/ ImageJ program. According to the Micro-CT analysis results of

Imagej program, the porosity volumes in the acidified region are ranging between 35-40%. Percentage change is 30-40% in the semi-acidified region, this value decreases and is between 20-45% in the non-acidified region. The porosity volumes are observed at least in the non-acidified region. It is seen that porosity is directly proportional with HCl acidizing.

4.5.1. Pore Perimeter Lengths

The number and perimeter lengths of porosity were measured in acidified, semi-acidified and non-acidified areas. As a result of the acidizing process, porosity numbers decreased by 28%, but the porosity perimeter lenghts increased. The 2995 pores were determined in the acidified sample using ImageJ/Analyze Particip measurement. The number ratio of pores is 38% (1130 pores) in the non-acidizing zone, 27% (813 pores) in semi-acidizing zone, 35% (1052 pores) in the acidizing zone. Small sized pores in non-acizing zone and semi-acidizing zone are not observed in the acidizing zone, there are larger pores joined with acid effect and therefore the number ratio of pores is low. The mean porosity perimeter lenght in the acidified region was 42.726 µm, whereas it was 39.069 µm and 31.514 µm in the semi-acidified and non-acidified regions, respectively.

Pore sizes vary according to regions and the change graph of this average perimeter length is given in Figure 7. In the regions where 15% diluted HCl acid effect was observed, no change was seen in small pores up to 20 µm length while pore perimeter values increased at 30 µm and more. The maximum increase is for the porosity with a perimeter greater than 120 µm.

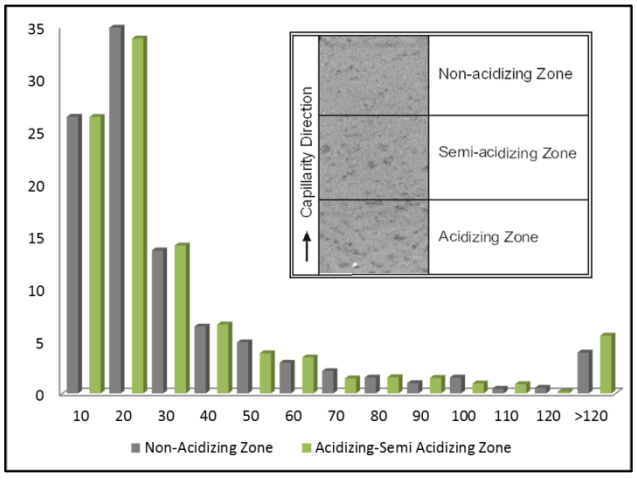

Figure 7. Change of porosity circumference lengths due to acidizing.

4.5.2. Pore-Throat

It has been observed that the distances between the pores observed in the dimensions of the pores and in connection with each other (pore throat) increased with acidification process. As a method, the associated pores were detected on the two-dimensional image of the acidified sample and the circles of the largest diameter that could fit into these pores were drawn. The distances between the two circles were measured and the lengths of the pore throat were determined (Freire-Gormaly, 2016). In the non-acidified sample, the area average of the pore throats is 3.875 μm^2, while it is 5.714 μm^2 in the semi-acidified region and 6.15 μm^2 in the acidified region, according to these results, the pore throat area increased to 58.7% by acidizing.

The average of perimeter lenght of the pore throat is 2.44 µm in the non-acidified region, 4.608 µm in the semi-acidified region and 5.004 µm in the acidified region, these results indicate that there is an increase of 105% by acidizing. In addition, the number of pore throats increased 2.5 times with acidizing.

5. DISCUSSION

The comparison of porosity with Micro-CT method and experimental methods has been studied by many researchers. Farokhiana et al., (2019) measured 16.03% of porosity experimentally in the Persian Gulf sandstones and 18.03% with Micro-CT. Churcher et al., (1991) reported that the porosity of Berea sandstones ranged from 19% to 26%, while Andrä et al., (2013) calculated 20% of the porosity of the sample with Micro-CT.

There are a limited number of studies investigating acidizing and porosity changes. Shafiq et al., (2013) observed changes in sandstones with 3% HF and 12% HCl acid and determined that the porosity change after the first acidizing was 47.08% and it was 63.91% in the after flush stage. Shafiq & Mahmud (2017) observed an increase of 10.10% porosity in the formation using HEDTA as acid in sandstones, an they observed 8.5% and 7.25% increases using EDTA and GLDA, respectively.

The porosity of the sandstones observed in Arsuz (Hatay) region was measured and the lithological properties were determined in this study. The effect of diluted HCl acid and capillarity of sandstones at different ratios and velocities and distances of water in pores were measured. Porosity changes by matrix acidizing was tested by using 7.5%, 15%, 30% HCl diluted acid solutions prepared for sandstone samples. Volumes of acid effect in the sample: 7.5%; 21.344 cm^3, 15%; 22.5 cm^3 and 30%; 51.75 cm^3. Total average porosity rate is 34.207%, and 36.546% in acided region, 34.649% in semi-acidizing region and 31.455% in non-acidizing sample. There is

an increase in the number of porosities with acidizing, as well as expansion and growth of existing pores. The mean porosity in the acidizing region was 42.726%, whereas it was 39.069 % and 31.514 % in the semi-acidizing and non-acidizing regions, respectively. It is possible to open or increase the pore throat by acidizing and the average of perimeter lenght of the pore throat in the non-acidizing, semi-acidizing and acidizing zone is 2.44, 4.61 and 5.00 µm, respectively. Pore perimeter lengths increased by about 105% with the effect of acidizing. Porosity values of the acidizing sample with 15% HCl were found to be 41% by Micro-CT and the porosity rate in the acidizing region was calculated as 42% in the 2D image analysis. The porosity value of the formation is determined as 40% by well logs; both methods show that the microporosity is consistent with the macroporosity values. Micro-CT and Image processing methods can be used instead of well logging to determine the porosity ratio more quickly.

6. CONCLUSION

In this paper, Micro CT-scans technique and the image analysis technique were employed to determine porosity distribution and average porosity of sandstones with different acid treatment. The image processing results were compared with Micro-CT result. Results from this study showed that the porosity calculated by CT-scan images is in a good agreement with experimental results obtained from sandstone, in addition to identifying the distribution of pores in non-destructive rock. It was observed in this study that porosity, pore throat values and changes in acid and micron size occur with large numerical differences. Depending on acid concentrations in future studies, micron-size pore studies of other commonly used acids will be useful in determining effective acid use in practice.

REFERENCES

Andrä, H., Combaret, N., Dvorkin, J., Glatt, E., Han, J., Kabel, M., & Marsh, M. 2013. *Digital rock physics benchmarks—Part I: Imaging and segmentation.* Computers & Geosciences, 50, 25-32.

Archie, G. E. 1950. *Introduction to petrophysics of reservoir rocks.* AAPG bulletin, 34(5), 943-961.

Cai, L., Guo, X., Zhang, X., Zeng, Z., Xiao, G., Pang, Y., & Wang, S. 2020. *Pore-throat structures of the Permian Longtan Formation tight sandstones in the South Yellow Sea Basin, China: A case study from borehole CSDP-2.* Journal of Petroleum Science and Engineering, 186, 106733.

Chen, Y., Jha, N. K., Al-Bayati, D., Lebedev, M., Sarmadivaleh, M., Iglauer, S., ... & Xie, Q. 2020. *Geochemical controls on wettability alteration at pore-scale during low salinity water flooding in sandstone using X-ray micro computed tomography.* Fuel, 271, 117675.

Churcher, P. L., French, P., Shaw, J. & Schramm, L. 1991. *Rock Properties of Berea Sandstone, Baker Dolomite, and Indiana Limestone.* SPE International Symposium on Oilfield Chemistry. Anaheim: Society of Petroleum Engineers, 431-446.

Cnudde, V., & Boone, M. N. 2013. *High-resolution X-ray computed tomography in geosciences: A review of the current technology and applications.* Earth-Science Reviews, 123, 1-17.

Desbois, G., Urai, J. L., Kukla, P. A., Konstanty, J., & Baerle, C. 2011. *High-resolution 3D fabric and porosity model in a tight gas sandstone reservoir: A new approach to investigate microstructures from mm-to nm-scale combining argon beam cross-sectioning and SEM imaging. Journal of Petroleum Science and Engineering*, *78*(2), 243-257.

Dong, H., & Blunt, M. J. 2009. *Pore-network extraction from micro-computerized-tomography images.* Physical review E, 80(3), 036307.

Farokhian, D., Azin, R., & Ranjbar, A. 2019. *Application of medical and dental CT-Scan technologies for determining porosity distribution of the Persian Gulf coastal zone and Zagros basin core samples.* Journal of African Earth Sciences, 150, 96-106.

Feng, X. T., Chen, S., & Zhou, H. 2004. *Real-time computerized tomography (CT) experiments on sandstone damage evolution during triaxial compression with chemical corrosion.* International Journal of Rock Mechanics and Mining Sciences, 41(2), 181-192.

Freire-Gormaly, M., Ellis, J. S., MacLean, H. L. & Bazylak, A. 2016. *Pore Structure Characterization of Indiana Limestone and Pink Dolomite from Pore Network Reconstructions.* Oil & Gas Science and Technology–Revue d'IFP Energies nouvelles, 71(3), 33.

Gao, H., Cao, J., Wang, C., He, M., Dou, L., Huang, X., & Li, T. 2019. *Comprehensive characterization of pore and throat system for tight sandstone reservoirs and associated permeability determination method using SEM, rate-controlled mercury and high-pressure mercury.* Journal of Petroleum Science and Engineering, 174, 514-524.

Grove, C. & Jerram, D. A. 2011. *jPOR: An ImageJ Macro to Quantify Total Optical Porosity from Blue-Stained Thin Sections.* Computers & Geosciences. 37(11), 1850-1859.

İztan H. & Harput, B. 1988. *Geochemical Analyses of Ten Cutting Samples from Iskenderun Sea -1 Well.* Turkish Petroleum Corporation (TPAO), Ankara, Report No. 1263.

Hillier, S. 1994. *Pore-lining chlorites in siliciclastic reservoir sandstones: electron microprobe, SEM and XRD data, and implications for their origin*. *Clay Minerals*, *29*(4), 665-679.

Kılınç, E. & Yeşilot Kaplan M. 2018. *Source Rock*

Characterictic of The Kızıldere Clays (Arsuz-Hatay). Cumhuriyet Science Journal, 39(2), 524-530.

Kılınç, E. & Yeşilot Kaplan, M. 2019. *Paleoenvironmental Conditions, Geochemistry and Hydrocarbon Pontential of Kızıldere Formation Hatay–Turkey*. Fresenius Environmental Bulletin, 28, 3519-3526.

Kozlu, H. 1987. Structural Development and Stratigraphy of Misis–Andirin Region. In Proceedings of the 7th Petroleum Congress of Turkey. Turkish Association of Petroleum Geologists., 104-116.

Kozlu, H. 1997. *Tectonic-Stratigraphic Units of Neogene Basins (İskenderun Misis-Andırın) in the Eastern Mediterranean Region and Their Tectonic Development*, Ankara University, Institute of Science and Technology, PhD Thesis, 188 p. (in Turkish with English summary)

Lai, J., Wang, G., Fan, Z., Chen, J., Wang, S., Zhou, Z., & Fan, X. 2016. Insight into the pore structure of tight sandstones using NMR and HPMI measurements. Energy & Fuels, 30(12), 10200-10214.

Larmagnat, S., Des Roches, M., Daigle, L. F., Francus, P., Lavoie, D., Raymond, J., ... & Aubiès-Trouilh, A. 2019. *Continuous porosity characterization: Metric-scale intervals in heterogeneous sedimentary rocks using medical CT-scanner*. Marine and Petroleum Geology, 109, 361-380.

Liu, M., Xie, R., Wu, S., Zhu, R., Mao, Z., & Wang, C. 2018. *Permeability prediction from mercury injection capillary pressure curves by partial least squares regression method in tight sandstone reservoirs.* Journal of Petroleum Science and Engineering, 169, 135-145.

Liu, X., Wang, J., Ge, L., Hu, F., Li, C., Li, X., ... & Xue, Q. 2017. *Pore-scale characterization of tight sandstone in Yanchang Formation Ordos Basin China using micro-CT and SEM imaging from nm-to cm-scale*. Fuel, 209, 254-264.

Moore, C. H., & Wade, W. J. 2013. *Carbonate reservoirs: Porosity and diagenesis in a sequence stratigraphic framework.* Newnes.

Peng, S., Hu, Q., Dultz, S., & Zhang, M. 2012. *Using X-ray computed tomography in pore structure characterization for a Berea sandstone: Resolution effect.* Journal of hydrology, 472, 254-261.

Schmidt, G.C. 1961. *Stratigraphic Nomenclature for the Adana Region Petroleum District.* VII. Petroleum Administration Bulletin, 6, 47-63.

Shabaninejad, M., Middlelton, J., & Fogden, A. 2018. *Systematic pore-scale study of low salinity recovery from Berea sandstone analyzed by micro-CT*. Journal of Petroleum Science and Engineering, 163, 283-294.

Shafiq H.K. & Mahmud, B. 2017. *Sandstone matrix acidizing knowledge and future development*. J Petrol Explor Prod Technol, pp. 1-12, 10.1007/s13202-017-0314-6.

Shafiq, M. U., Shuker, M. T., & Kyaw, A. 2013. *Performance prediction of acids on sandstone acidizing.* ASJ Int J Adv Sci Res Rev (IJASRR), 1(2), 07-12.

Tekin, E., Varol, B., & Ayyıldız, T. 2010. *Sedimentology and Paleoenvironmental Evolution of Messinian Evaporites in the İskenderun-Hatay Basin Complex, Southern Turkey*. Sedimentary Geology, 229/4, 282-298.

Tendam, A. 1951. *Sedimentation and Facies in*. Geology Bulletin Turkey, 2, 5-66. Ankara. (in Turkish)

Wang, G., Chang, X., Yin, W., Li, Y., & Song, T. 2017. *Impact of diagenesis on reservoir quality and heterogeneity of the Upper Triassic Chang 8 tight oil sandstones in the Zhenjing area, Ordos Basin, China*. Marine and Petroleum *Geology*, *83*, 84-96.

Wyllie, M. R. J., & Rose, W. D. 1950. *Some theoretical considerations related to the quantitative evaluation of the physical characteristics of reservoir rock from electrical log data.* Journal of Petroleum Technology, 2(04), 105-118.

Xi, K., Cao, Y., Haile, B. G., Zhu, R., Jahren, J., Bjørlykke, K., ... & Hellevang, H. 2016. *How does the pore-throat size control the reservoir quality and oiliness of tight sandstones? The case of the Lower Cretaceous Quantou Formation in the southern Songliao Basin, China. Marine and Petroleum Geology*, *76*, 1-15.

Yalcin, M. G., Coskun, B., Nyamsari, D. G., & Yalcin, F. 2019. *Geomedical, ecological risk, and statistical assessment of hazardous elements in shore sediments of the Iskenderun Gulf, Eastern Mediterranean, Turkey.* Environmental Earth Sciences, 78(15), 438.

Yang, S.Q., Huang, Y.H., Jing, H.W. & Liu, X.R. 2014. *Discrete Element Modeling on Fracture Coalescence Behavior of Red Sandstone Containing Two Unparallel Fissures Under*. Engineering Geology. 178, 28-48.

Yang, Y., Li, Y., Yao, J., Zhang, K., Iglauer, S., Luquot, L., & Wang, Z. 2019. *Formation damage evaluation of a sandstone reservoir via pore-scale X-ray computed tomography analysis.* Journal of Petroleum Science and Engineering, 183, 106356.

Yuan, B., Chareyre & Darve, F. 2015. *Pore-Scale Simulations of Drainage in Granular Materials, Finite Size Effects and the Representative Elementary Volume*. Advances in Water Resour. 95, 109–124.

Received at: 05. 09. 2020
Revised at: 23. 10. 2020
Accepted for publication at: 30. 12. 2020
Published online at: 07. 01. 2021